This is a preprint, the final version is subject to change, of the American Mineralogist (MSA)
Cite as Authors (Year) Title. American Mineralogist, in press.
(DOI will not work until issue is live.) DOI: http://dx.doi.org/10.2138/am.2013.4372

Revision 3

Synthesis and characterization of kanemite from fluoride-containing media: Influence of the alkali cation

JUAN I. CORREDOR[1], AGUSTÍN COTA[2,4], ESPERANZA PAVÓN[3]

AND MARIA D. ALBA[4†]

[1] Unidad de RMN-SCAI. Campus de Rabanales. Edificio Ramón y Cajal.

Universidad de Córdoba, 14071-Córdoba (SPAIN)

[2] Laboratorio de Rayos-X. CITIUS. Universidad de Sevilla.

Avda. Reina Mercedes, 4b. 41012-Sevilla (SPAIN)

[3] Unité de Catalyse et de Chimie du Solide, UCCS, CNRS, UMR8181,

Université Lille Nord de France, 59655 Villeneuve d'Ascq (FRANCE)

[4] Instituto Ciencia de los Materiales de Sevilla

Consejo Superior de Investigaciones Científicas-Universidad de Sevilla,

Avda. Americo Vespucio, 49, 41092 Seville (SPAIN)

ABSTRACT

Kanemite belongs to the group of sodium silicate minerals that it is a naturally occurring mineral first found in Kanem, at the edge of the Lake Chad, and has been synthesized in different ways from NaOH-SiO_2 mixtures and used as precursor for the design of microporous and mesoporous materials. The fluoride route to the synthesis of microporous materials is based on the substitution of OH^- anions by fluoride anions, which may subsequently also play a mineralizing role, and gives rise to materials with higher hydrophobicity and thermal and hydrothermal stability. Moreover, F^- plays an important role in the incorporation of framework heteroatoms, thereby affecting the activity of the final material. The aim of this study was to synthesize fluorokanemite using different synthetic routes and different F^- source. The final product was characterized by a combination of

† E-mail: alba@icmse.csic.es.

methods that provided information regarding the incorporation of fluorine into the framework and the short- and long-range structural order of the fluorosilicate. Kanemite with water content close to ideal was obtained in all cases. The washing process was found to have no effect in the long- or short-range structural order of the layer framework, although it did affect the structure of the cation in the interlayer space of kanemite. The mineralizing agent therefore appears to be the key to the synthesis. Furthermore, it governs the resulting kanemite structure by controlling the formation of hydrogen bonds in the framework, and therefore the degree of lamellar structure condensation.

Keywords. kanemite, mesoporous, microporous, fluorosilicates, MAS NMR, DRX, mineralizing agent, FSM-16.

INTRODUCTION

The fluoride route to the synthesis of microporous materials is based on the substitution of OH^- anions by fluoride anions, which may subsequently play a mineralizing role. This procedure has been widely used for the synthesis of several zeolites, clathrasils, and phosphates (Gurth et al., 1993; Kessler et al., 1994; Camblor et al., 1996, 1997b, 1997c), and has allowed the optimal incorporation of heteroatoms such as Al or B into them (Guth et al., 1986).

Kimura and Kuroda (2009) pointed out relevance of a synthetic strategy of ordered mesoporous silica derived from layered silicates composed of single silicate sheets for synthesizing crystalline, ordered mesoporous silica, which has not yet been achieved. Moreover, the incorporation of various metal species in the starting layered silicates is also important for extending the catalytic applications of ordered mesoporous silica. In this way, zeolite beta, when synthesized in a F^- medium, exhibited a higher hydrophobic character than the material synthesized in a basic medium, and this has been shown to be beneficial for its

catalytic activity and selectivity in reactions involving molecules with different polarities (Camblor et al., 1997a; Blasco et al., 1998). Perez-Romo et al. (2003) have demonstrated that the presence of fluoride anions during the synthetic cation-exchange process that leads to FSM-16 gives rise to an increased wall thickness, thus explaining the greater thermal stability of this material (Perez-Romo et al., 2005). Fluoride ions are also known to influence the nature, activity and polymerization activity of silica precursors and a fluorinated silica surface is much more hydrophobic and more resistant to the attack of water molecules than a silanol silica surface (Brinker et al., 1990). More recently, Kim et al. (2001) have reported that the hydrothermal stability of MCM-48 can be improved by post-treatment in NaF solution.

Crystallization patterns and crystal morphologies are also influenced by the addition of fluoride salts, generally HF or NH_4F, to the reaction mixture as a source of F^- ions (Gabelica et al., 1992, 1993; Kessler et al., 1994). The NH_4-containing system is the most effective for the incorporation of gallium into the MFI framework, whereas the Na- and Cs-containing systems have been shown to be the least effective. The influence of the cations may vary depending on either the induction rate or the crystal growth rate (Nigro et al., 1999). In this respect, kinetic data have shown that alkali-metal cations exert both electrostatic and specific effects during stabilization of the first nuclei and the tiny growing crystals. Furthermore, an evaluation of the thermal stability of BEA zeolites synthesized with and without NH_4F has shown that the thermal stability of the former is relatively higher than that of the latter (Jon et al., 2006).

Layered sodium silicates such as kanemite, ilerite and magadiite are interesting materials owing to their ion-exchange and intercalation properties (Lagaly et al., 1975). These interesting features of layered silicates have paved the way for their use as precursors for the synthesis of silica-pillared ilerite (Kosuge and Tsunashima, 1995) and mesoporous materials, such as FSM-16, KSW-1 and KSW-2, with high BET surface areas, narrow pore-size

distributions and higher stability than similar silicates synthesized by hydrothermal or sol-gel methods (Yanagisawa et al., 1990; Kimura et al., 2000). Furthermore, the transformation and/or recrystallization of layered sodium silicates, especially kanemite, into several known zeolites have been well documented in the literature (Pál-Borbély et al., 1997, 1998, 2000; Feng and Balkus, 2004). The use of the kanemite as a precursor for the synthesis of mesoporous and microporous silicates via the fluorine route will therefore improve their properties, although this requires the synthesis of fluorokanemite.

The aim of this study was to synthesize fluorokanemite using different synthesis routes with either NaF or NH_4F as the F^- ion source. The final product was characterized by a combination of methods that provided information regarding the efficiency of fluorine incorporation into the framework and the short- and long-range structural order of the layered fluorosilicate.

EXPERIMENTAL METHODS

Synthesis of fluorokanemites

Layered fluorokanemites were prepared by dissolution of appropriate amounts of sodium and/or ammonium, the molar ratio Si: mineralizing cations was kept constant and equal to one [$Si/(Na+NH_4)=1$; see Table 1], in 50 g of a sodium silicate solution (ALDRICH, 12.6% Si, 13.8% NaOH). The reaction mixtures were heated at 100 °C for 72 h in an open crucible and the resulting products calcined at 700 °C for 6 h. After cooling to room temperature, the solids were dispersed in 20 times their weight of water and stirred for 15 minutes. The silicate was recovered by filtration, washed with distilled water, NaF or NH_4F solution (solution/solid=10 wt%; see Table 1), then dried in air at room temperature (Alba et al., 2006). Samples will hereinafter be referred to as detailed in Table 1.

Sample Characterization.

Thermogravimetric (TG) analyses were performed using a TA (SDT-Q600) instrument to determine the amount of residual water. The sample temperature was increased to 900 °C at a rate of 10 °C·min^{-1} in air.

X-ray diffraction (XRD) patterns were recorded at the X-ray Laboratory of CITIUS (University of Seville, Spain), using a D8 Advance Bruker instrument equipped with a Cu Kα radiation source, operating at 40 kV and 40 mA, and a graphite monochromator. Diffractograms were obtained from 3° to 120° 2θ with a step size of 0.02° 2θ and a time step of 10.0 s. Crystalline phase identification was carried out using the DIFFRAC^{plus} Evaluation package (Bruker, 2010).

The sample morphology was analyzed using a scanning electron microscope (JEOL, Model JSM-5400) at 20 kV at the Microscopy Service of the Instituto Ciencia de los Materiales de Sevilla (CSIC-US, Seville, Spain). An energy dispersive X-ray (EDX) system (Oxford Link ISIS) was fitted to the SEM equipment to perform chemical analysis of the samples using a Si/Li detector with Be window.

FTIR spectra were recorded in the the Spectroscopy Service of the ICMS (CSIC-US, Seville, Spain), as KBr pellets, using a Nicolet spectrometer (model 510P) with a nominal resolution of 4 cm^{-1}.

Single-pulse (SP) MAS-NMR spectra were recorded at the Spectroscopy Service of SCAI (University of Cordoba, Spain) using a Bruker AVANCE WB400 spectrometer equipped with a multinuclear probe. Powdered samples, at the hydration state described in the TG section (Table 2), were packed in 4 mm zirconia rotors and spun at 12 kHz. ^{1}H MAS spectra were obtained using typical π/2 pulse widths of 4.25 μs and a pulse space of 5 s. ^{29}Si MAS NMR spectra were acquired at a frequency of 79.49 MHz, using a pulse width of 1.4 μs (π/2 pulse length = 4.2 μs) and a delay time of 300 s. ^{19}F MAS NMR spectra were acquired at

a frequency of 376.50 MHz, using typical π/2 pulse widths of 4.0 μs and a delay time of 5 s, and the rotor was spun at 20 kHz. The chemical shift values are reported in ppm with respect to tetramethylsilane for ^{1}H and ^{29}Si and NaF for ^{19}F.

^{1}H→^{29}Si cross-polarization experiments were performed under MAS conditions with high power proton decoupling using a single contact. Spectra were acquired using a ^{1}H π/2 pulse of 2.1 μs and an optimized contact time of 3.5 ms. The Hartmann-Hahn condition was established using the standard sample kaolinite.

^{23}Na 2D MQMAS spectra were recorded using a three-pulse sequence (5, 2.2 and 12 μs), a Z-filter (Amoureux et al., 1996), and rotation-synchronized acquisition at a sample spinning rate of 12 kHz. The chemical shift values are reported in ppm with respect to 1 M NaCl.

RESULTS AND DISCUSSION

The TG curves (Suppl. 1) show a four-step dehydration process: step A up to 105 °C, step B from 105 to 159 °C, step C from 159 to 216 °C and step D from 216 to 325 °C. The TG data are summarized in Table 2. The amount of water is expressed by *x* in the form $NaHSi_2O_5 \bullet xH2O$; note that the amount of hydroxyl groups is evaluated in the form of H_2O. Beneke and Lagaly (1977) have suggested the presence of two types of water in the interlayer space of kanemite, with one type forming an interlamellar monolayer of water molecules and the other being trapped within vacancies of the folded SiO_3OH hexagonal rings. Additional water molecules are adsorbed on the external surface or in the crystalline region, with hydroxyl groups being the source of the evolved water. Each step in the TG curve cannot be assigned exclusively to one particular species. Thus, the surface water and interlamellar water are released in step A, water within the hexagonal rings may be released in steps B and C and some of the hydroxyl groups are released in step D (Hayashi, 1997).

Kanemites synthesized using NaOH as mineralizing agent (K01 and K01F) have a total x value of around 3.18, compared with 3 for an ideal composition (Beneke and Lagaly, 1977). Both, the nature of the mineralizing agent and washing procedure have a marked influence on the final value of x, which is lower when NaF or NH_4OH are used as mineralizing agent. The lowest value of x is observed when NH_4F is used.

Figure 1 shows the X-ray diffraction pattern of all the kanemite samples synthesized as well as the silicate structure. The initial pattern, for K01 (Figure 1a), is consistent with crystalline kanemite (PDF file number 25-1309). Thus, the peak at $2\theta=8.65°$ is assigned to the (020) reflexion and indicates a basal spacing of 1.02 nm, as previously reported by Johan and Maglione (1972) for purely siliceous kanemite. Additionally, the weak peak observed at $2\theta=9.30°$ can be assigned to another (020) reflexion with a basal spacing of 0.95 nm. No reflexions for other phases are observed. In general, the intensity and position of the (020) reflexion are not affected by the washing process; sample K01F shows a similar diffraction pattern.

The use of NaF or NH_4OH as mineralizing agent results in a decreased intensity of the kanemite (020) reflexion, with this decrease being more marked when NH_4OH is employed, and the appearance of new reflexions due to cristobalite (PDF 39-1425) and low-tridymite (PDF 42-1401). Finally, the use of NH_4F as mineralizing agent provokes a drastic intensity decrease for the kanemite reflexions and the appearance of a new (020) reflexion with a basal spacing of 1.3 nm. This layer expansion cannot be explained on the basis of the amount of water in the structure, which decreases drastically, but may instead be due to an increased number of framework interconnections giving rise an expansion in the b-dimension.

The microstructural analysis of the particles (Figures 2 and 3) shows that samples K01 and K01F (Figures 2a and 2b) contain particles with a lamellar morphology typical of kanemite (Alba et al., 2010) and that this morphology is not affected by the washing process.

The EDX spectra (Suppl. 2) showed a Si/Na ratio similar in those samples. However, the use of mineralizing agents other than NaOH results in a smaller lamellar particle size with a higher Si/Na ratio (see EDX spectra in Suppl. 2) and the appearance of additional compacted particles that may be compatible with the presence of the cristobalite and tridymite phases already observed by XRD.

The ^{29}Si (SP) MAS NMR spectra of K01 and K01F (Figure 4a, solid line) show a signal at –97.3 ppm, which is assigned to Q^3($Si(OSi)_3OH$) environment (Lippman et al., 1980). A similar value has been reported previously by Pinnavaia and Johnson (1986). This result supports the single-layered silicate structure of kanemite and that the structure contains undistinguishable siloxide and silanol Q^3 silicon atoms. However, these two species would not be expected to have overlapping ^{29}Si NMR signals [a semi-empirical study (Janes and Olfield, 1985) predicts a chemical shift difference of 3.5 ppm between $(SiO)_3SiONa$ and $(SiO)_3SiOH$] due to the existence of hydrogen bonds between the Q^3 silicon atoms of the silicates. To corroborate that, ^{29}Si (CP) MAS NMR experiments were carried out and are plotted in Figure 4 (dashed lines).

The CP spectra for K01 and K01F (Figures 4a and 4b, dashed line) show a signal that is well-resolved into four signals at –95.9, –97.3, –98.5 and –99.1 ppm, thus indicating a contribution from ^{1}H dipolar interactions (Hayashi, 1997). The presence of several signals has been explained in the literature as being due to different mean Si-O-Si angles, with a higher frequency shift implying a smaller mean Si-O-Si angle and shrinkage of the SiO_4 network (Thomas et al., 1983; Ramdas and Klinowski, 1984). The doublet observed at around –105 ppm could be due to silanol groups in a higher condensed state.

The ^{29}Si (SP) MAS NMR spectra of the kanemite synthesized using NaF, NH_4OH or NH_4F as mineralizing agent (Figures 4a and 4b) shows a further peak at –109.2 ppm, which was assigned to Q^4 species in cristobalite and tridymite (Hayashi, 1997). Synthesis in the

presence of these mineralizing agents results in interlayer condensation and the formation of 3D silicates (it favored the Si-O-Si condensation), with the proportion of Si Q^4 environments being inversely proportional to the water content (% w/w) determined by TG from the weigh loss up to 325º C, as can be seen from Figure 4c (R^2=9.674). Additionally, the spectrum of K01NF (Figure 4b) shows a signal at –101.9 ppm due to Q^4(3Si, 1OH) (Engelhardt and Michel, 1987), and that for FK01NF (Figure 4b) shows two small signals at –86.3 and –88.2 ppm due to β-$Na_2Si_2O_5$ (Mackenzie and Smith, 2002), which has previously been observed as an impurity in kanemite (Alba et al., 2006). Taking into account the percentage of Si responsible for each ^{29}Si signal in the ^{29}Si (SP) MAS NMR spectra, the total *x*-value can be recalculated with respect to the amount of kanemite, which is the only hydrated species present (see last column Table 2). These recalculated total *x* values are in the range 2.62–3.62. The high total *x* values calculated for the samples with a Si/(Na+NH_4) ratio of one synthesized in a fluoride medium could explain the high value of the b parameter (interlayer distance, Figure 1c) observed by XRD.

The ^{1}H MAS NMR spectra of K01 and K01F (Figure 5a) show two types of signals at around 15.5 (signal I) and 5.3 ppm (signal II), which can be assigned to hydroxyl groups and water molecules, respectively (Hayashi, 1997). When NaF is used as mineralizing agent, a new signal, which is due to isolated silanol protons, appears at around 1.5 ppm (signal III) (Mackenzie and Smith, 2002). Although these contributions also appear in the kanemites with Si/(Na+NH_4)=1, more complex behavior is observed in these silicates. Thus, whereas the water signal (signal II) is symmetric and centered at 5.5 ppm for K01, for the samples synthesized in a fluoride medium (K01F, FK01 and FK01F) it is asymmetric due to the overlap of two signals. This could be explained by the presence of two different coordination spheres for Na, in one of which some of the water molecules have been substituted by F. Likewise, for the sample synthesized with NaF as mineralizing agent (FK01 and FK01F),

signal I results from the overlap of two signals, one at 15.5 ppm and other at 16.5 ppm (FK01) or 17.9 ppm (FK01F). A previously observed high frequency shift of strongly hydrogen-bonded protons has been related to the oxygen-oxygen distance of the O···H···O bond such that a shorter distance is correlated with a higher frequency (Eckert et al., 1988). The peak at 16.5 ppm can therefore be assigned to a strongly hydrogen-bonded proton. The chemical shift can be related to the oxygen-oxygen distance of the $^{-}$O···H···O^{-} bond (d) using the empirical equation derived by Eckert et al. (1988): δ_H=79.05 – 0.255d/pm. For the chemical shifts reported here (δ_H=15.5 and 16.5 ppm), this gives d values of 249.2 and 245.3 pm, respectively. The use of NaF therefore results in a shorter hydrogen bond distance, which could explain the high condensation degree of tetrahedral silicon observed herein (see Figure 4).

The IR/FT spectra (Figure 6) show similar results in the region of stretching vibration of OH groups of water molecules, region 3700-3000 cm^{-1}, (Lazarev, 1972). In this region two set of bands are observed (Huang et al., 1999): a relative sharp peak at higher frequency ca. 3591 cm^{-1}, due to isolate OH groups, and, two broad bands at lower frequencies (3255 and 3400 cm^{-1}), related to the OH groups involved in interlayer hydrogen bond. The presence of those signals are agreed with the observed OH environments (signals I and III) in the ^{1}H MAS NMR spectra.

The ^{1}H MAS NMR spectra of the samples synthesized with Si/(Na+NH_4)=1 (Figure 5b) are more complex, with three new sets of signals appearing at around 10 (signal IV, due to NH_4^+) (Del Bene et al., 1990), 0.7 and –2.0 to –14.5 ppm (signal V and VI, due to free and encapsulated NH_3, respectively) (Haase and Sauer, 1994; Wang et al., 2009). The water signal (signal II) is an overlap of four signals ranging between 3.5 and 6.8 ppm as a consequence of the simultaneous presence of Na^+ and NH_4^+ in the interlayer space. A similar phenomenon has previously been observed in layered aluminosilicates and correlated to the acidic properties of

those silicates (Alba et al., 2000; Alba et al. 2003). Finally, signal I is composed of a set of three or four signals in the range 13.6–21.2 ppm, possibly due to the presence of more than one hydrogen bond between OH, F or NH_3 groups.

The intensity ratio between signals I and II has been plotted in Figure 5c as function of the synthetic conditions. It is clear from this plot that, for the kanemite with Si/Na=1, the amount of hydrogen bonds increases when using NaF rather than NaOH as mineralizing agent and that this increase is higher still when the sample is washed with a fluoride medium. Same trend has been observed in the OH region between 3400-3200 cm^{-1} of the IR/FT spectra (Figure 6a). In contrast, for the kanemite with Si/(Na+NH_4)=1, the amount of hydrogen bonds remains almost constant upon varying the synthetic conditions, although it is higher than for the sample with Si/Na=1 in all cases except FK01NF.

All ^{19}F peaks (Figure 7) are Lorentzian in shape, possibly indicating some type of motion of the fluoride anion that results in partial averaging of homo- or heteronuclear dipolar broadening (Kiczenski and Stebbins, 2002). All spectra, except of FK01, show a signal at –223.9 ppm which is nearly identical in position to that of crystalline NaF (Schaller et al., 1992; Miller, 1996), but is much broader, thus indicating the absence of this phase itself but the presence of F groups that most likely have the same coordination number at Na (six) (Zeng and Stebbins, 2000).

In the spectra of FK01 and FK01F, a small signal is observed at ca. -107 ppm that could be interpreted as being due to the presence of non-specifically adsorbed F^- (O-H···F) (Arens et al., 1984).

In the spectra of the three kanemites with Si/(Na+NH_4)=1, other intense and narrow signal is observed at -122.4 ppm. Delmotte et al. (1990), who used ^{19}F NMR spectroscopy to study crystalline microporous alumino- and gallosilicates synthesized in a fluoride-containing medium, observed that the spectra contained a resonance at –129 ppm assigned to Si-F

species. On the other hand, the sharp peak observed at –123 ppm for SBA samples was assigned to the presence of the F^- counterion of NH_4^+ or H^+ in the channels of the zeolites (Delmonte et al., 1990; Guth et al., 1992). The signal observed at –121.7 ppm must therefore be due to the presence of the F^- counterion of Na^+ and/or Si-F species. Additionally, K01NF and FK01NF, show a small signal at -189.4 and -211.7 ppm, respectively. The signal at -189.4 ppm should be due to the SiF_6 species (Zeng and Stebbins, 2000) and the signal at -211.7 ppm has not been possible to be assigned.

In order to gain a better understanding of the interlamellar cation, ^{23}Na 3Q MAS NMR spectra were recorded. Figure 8 shows the 2D spectrum obtained for K01 as an example. Once the different Na sites had been identified from the 2D spectra, this information was used to simulate the 1D spectra. The results of these simulations are summarized in Tables 3 and 4. The ^{23}Na 3Q MAS NMR spectrum of K01 (Figure 8) consists of two components with small and large quadrupole interactions, respectively. Using this information to simulate the 1D spectrum (not shown) gives a main contribution (82%) from a signal with δ_{iso}=2.58 ppm, χ=1.96 MHz and η_Q=0.81 and another signal with δ_{iso}=–0.59 ppm, χ=0.478 MHz and η_Q=0.10, as previously reported for kanemite (Hayashi et al., 1997). The first of these signals (δ_{iso}=2.58 ppm) was assigned to Na^+ species that have a fixed orientation rather than rotating isotropically. The water molecules are not coordinated to these Na^+ species directly (Hayashi et al., 1997). This kind of Na^+ predominates in all samples with the exception of FK01NF. For kanemites with Si/Na=1 synthesized in a fluoride medium, this signal is the overlap of two signals ranging between 3.1 and 1.76 ppm due to the influence of F^- in the coordination sphere. Similar results are observed for the kanemites with Si/(Na+NH_4)=1, although δ_{iso} is shifted by 0.4 ppm to lower frequency, probably due to the simultaneous presence of NH_4^+. In a previous study, Hanaya and Harris (1998) observed several signals with $\delta_{iso}\geq$0 ppm that were assigned to hexacoordinated sodium ions. Part of this coordination was assigned to O

and part to H_2O (3 or 4), therefore the octahedral coordination structures of such sodium ions are expected to be rather distorted, as can be seen from the χ and η values. In this case, the interlamellar Na forms an inner-sphere complex.

The other components with $\delta_{iso}<0$ ppm are due to Na^+ species directly coordinated by water molecules. The excess water molecules provide a higher local symmetry in this outer-sphere complex (Hanaya and Harris, 1998). At this respect, it should be noted that this is the only kind of Na^+ species in FKO1F.

CONCLUSIONS

Kanemite with a water content close to the ideal value [$NaHSi_2O_5 \cdot xH_2O$ (x=2.62–3.61)] was obtained by all synthetic routes. The washing process did not affect the long- and short-range structural framework. However, washing was found to affect the structure of the cation in the interlayer space of kanemite, as demonstrated by ^{1}H MAS and ^{23}Na MQ MAS NMR spectroscopy. The nature of the mineralizing agent was found to be the key to the synthesis and to affect the structure of the resulting kanemite, and therefore the degree of lamellar structure condensation, by governing the formation of hydrogen bonds in the framework.

Although the nature of the interlayer cation (Na^+ with NaOH or NaF, and a mixture of Na^+ and NH_4^+ with NH_4OH or NH_4F) depends on the mineralizing agent, the hydration state and the chemical nature of the coordination sphere of the interlayer cation depend on the reaction medium. Thus, when the medium contains fluoride the interlayer cation is partially coordinated by fluorine. Moreover, two different coordination spheres have been detected for interlamellar Na, which forms an outer-sphere complex at one site and an inner-sphere complex at the other.

Finally, hydrogen bonds of different strengths and involving different electronegative groups have been detected as a function of the synthetic conditions. Thus, for the kanemite with Si/Na=1, the amount of hydrogen bonds is higher when NaF is used as mineralizing agent than with NaOH, and this increase is higher still when the sample is washed with a fluoride medium. In the case of the kanemite with Si/(Na+NH_4)=1, the amount of hydrogen bonds remains almost constant upon varying the synthetic conditions, although it is higher than for all samples with Si/Na=1 synthesized under similar conditions except FK01NF.

ACKNOWLEDGMENTS

We would like to thank the DGICYT and FEDER funs (project no. CTQ 2010-14874) for their financial support.

REFERENCES CITED

Alba, M.D., Becerro, A.I., Castro, M.A. and Perdigon, A.C. (2000) High-resolution H-1 MAS NMR spectra of 2:1 phyllosilicates. Chemical Communications, 37-38.

Alba, M.D., Becerro, A.I., Castro, M.A., Perdigon, A.C. and Trillo, J.M. (2003) Inherent acidity of aqua metal ions in solids: An assay in layered aluminosilicates. Journal of Physical Chemistry B, 107, 3996-4001.

Alba, M.D., Chain, P., Pavon, E. (2006) Synthesis and characterization of gallium containing kanemite. Microporous and Mesoporous Materials, 94, 66-73.

Alba, M.D., Castro, M.A., Chain, P., Orta, M.M., Pazos, M.C. and Pavon, E. (2010) Hydrothermal stability of layered silicates in neutral and acidic media: effect on engineered-barrier safety. Clays and Clay Minerals, 58, 501-514

Amoureux, J.P., Fernandez, C., Steuernagel, S. (1996) Z filtering in MQMAS NMR. Journal of Magnetic Resonance A, 123, 116-118

Arends, J., Nelson, D.G.A., Dukman, A.G. and Jongebloed, W.L. (1984) in Cardiology Today (B. Guggenheun, Ed.), pp. 245-258

Blasco, T., Camblor, M.A., Corma, A., Esteve, P., Guil, J.M., Martínez, A., Perdigón-Melón, J.A. and Valencia, S. J. (1998) Direct synthesis and characterization of hydrophobic aluminum-free Ti-beta zeolite. Journal of Physical Chemistry B, 102, 75-88.

Beneke, K. and Lagaly, G. (1977) Kanemite - inner-crystalline reactivity and relations to other sodium silicates. American Mineralogist, 62, 763-771

Brinker, C.J. and Scherer, G.W. (1990) Sol–Gel Science, Academic Press, London, p. 107, 644

Camblor, M.A., Corma, A. and Valencia S. (1996) Spontaneous nucleation and growth of pure silica zeolite-beta free of connectivity defects. Chemical Communications, 2365-2366

Camblor, M.A., Corma, A., Iborra, S., Miquel, S., Primo, J. and Valencia, S. (1997a) Beta zeolite as a catalyst for the preparation of alkyl glucoside surfactants: The role of crystal size and hydrophobicity. Journal of Catalysis, 172, 76-84

Camblor, M.A., Corma, A., Lightfoot, P., Villaescusa, L.A. and Wright, P.A. (1997b) Synthesis and structure of ITQ-3, the first pure silica polymorph with a two-dimensional system of straight eight-ring channels. Angewandte Chemie International Edition, 36, 2659-2661.

Camblor, M.A., Corma, A. and Villaescusa, L.A. (1997c) ITQ-4: A new large pore microporous polymorph of silica. Chemical Communications, 749-750

Del Bene, J.E., Perera, S.A. and Bartlett, R.J. (1999) Hydrogen bond types, binding energies, and (1)H NMR chemical shifts. Journal of Physical Chemistry A, 103, 8121-8124.

Delmotte, L., Soulard, M., Guth, F., Seive, A., Lopez, A. and Guth, J.L. (1990) 19F MAS NMR-studies of crystalline microporous solids synthesized in the fluoride medium. Zeolites, 10, 778-783.

Eckert, H.Y., Yesinowski, J., Silver, L.A. and Stolper, E.M. (1988) Water in silicate-glasses - quantitation and structural studies by H-1 solid echo and MAS-NMR methods. Journal of Physical Chemistry, 92, 2055-2064.

Engelhardt, G. and Michel, D. (1987) High Resolution Solid State NMR of Silicates and Zeolites; Wiley: New York.

Feng, F. and Jr. Balkus, K.J. (2004) Recrystallization of layered silicates to silicalite-1. Microporous and Mesoporous Materials, 69, 85-96.

Gabelica, Z., Mayenez, C., Monque, R., Galiasso, R., Giannetto, G., Occelli, M.L. and Robson, H.E. editors (1992). Molecular by the electrostatic stabilization of the double Sieves Vol. I , Van Nostrand, New York, , p. 190

Gabelica, Z., Giannetto, G., Dos Santos, F., Monque, R. and Galiasso, R. in: R. von Ballmoos et al. (Eds.), Proc. 9th Int. Zeolite Conf., Butterworth-Heinemann, Stoneham, 1993, p. 231. Part I.

Guth, J.L., Kessler, H. and Wey, R. (1986) New Route to Pentasil-Type Zeolites Using a Non Alkaline Medium in the Presence of Fluoride Ions. Studies in Surface and catalysis, 28, 121-128

Guth, J.L., Delmotte, L., Soulard, M., Brunard, N., Joly, J.F. and Espinat, D. (1992) Synthesis of Al,Si-MFI-type zeolites in the presence of F-anions - structural and physicochemical characteristics. Zeolites, 12, 929-935

Guth, J. L, Kessler, H., Caullet, P., Hazm, J., Merrouche, A. and Patarin, J. (1993) in Proc. Ninth Int. Zeolite Conf., ed. R. von Ballmoos, J. B. Higgins and M. M. J. Treacy, Butterworth, Heinemann, , p. 215

Haase, F. and Sauer, J. (1994) H-1-NMR chemical-shifts of ammonia, methanol, and water-molecules interacting with bronsted acid sites of zeolite catalysts - ab-initio calculations. Journal of Physical Chemistry, 98, 3083-3085.

Hanaya, M. and Harris, R.K. (1998) Two-dimensional Na-23 MQ MAS NMR study of layered silicates. Journal of Materials Chemistry, 8, 1073-1079.

Hayashi, S. (1997) Solid-state NMR study of locations and dynamics of interlayer cations and water in kanemite Journal of Materials Chemistry, 7, 1043-1048.

Huang, Y., Jiang, Z. and Schwiege, W. (1999) Vibrational Spectroscopic Studies of Layered Silicates, Chemistry of Materials, 11, 1210-1217.

Inagaki, S., Fukushima, Y. and Kuroda, K. (1993) Synthesis of highly ordered mesoporous materials from a layered polysilicate. Chemical Communications, 680-682

Janes, N. and Oldfield, E. (1985) Prediction of Si-29 nuclear magnetic-resonance chemical-shifts using a group electronegativity approach - applications to silicate and aluminosilicate structures. Journal of the American Chemical Society, 107, 6769-6775.

Johan, Z. and Maglione, G.F. (1972) Kanemite, a new hydrated sodium silicate. Bulletin de la Societe Francaise Mineralogie et de Cristallographie, 95, 371-&.

Jon, H., Lu, B., Oumi, Y., Itabashi, K. and Sano, T. (2006) Synthesis and thermal stability of beta zeolite using ammonium fluoride. Microporous and Mesoporous Materials, 89, 88-95.

Kessler, H., Patarin, J. and Schott-Darie, C. (1994) The opportunities of the fluoride route in the synthesis of microporous materials. Studies in Surface Science and Catalysis, 85, 75-113

Kiczenski, T.J. and Stebbins, J.F. (2002) Fluorine sites in calcium and barium oxyfluorides: F-19NMR on crystalline model compounds and glasses. Journal of Non-Crystalline Solids, 306, 160-168.

Kim, W.J., Yoo, J.C. and Hayhurst, D.T. (2001) Synthesis of MCM-48 via phase transformation with direct addition of NaF and enhancement of hydrothermal stability by post-treatment in NaF solution. Microporous and Mesoporous Minerals, 49, 125-137.

Kimura, T., Kamata, T., Fuziwara, M., Takano, Y., Kaneda, M., Sakamoto, Y., Terasaki, O., Sugahara, Y. and Kuroda, K. (2000) Formation of novel ordered mesoporous silicas with square channels and their direct observation by transmission electron microscopy. Angewandte Chemie International Edition, 39, 3855.

Kimura, T. and Kuroda, K. (2009). Ordered mesoporous silica derived from layered silicates. Advanced Functional Materials, 19, 511-527.

Kosuge, K. and Tsunashima, A. (1995) New silica-pillared material prepared from the layered silicic-acid of ilerite. Chemical Communications, 2427-2428.

Lagaly, G., Beneke, K. and Weiss, A. (1975) Magadiite and H-Magadiite .1. Sodium magadiite and some of its derivatives. American Mineralogist, 60, 642-649.

Lazarev, N. Vibrational Spectra and Structure of Silicates; Consultants Bureau: New York, 1972

Lippman, E., Maegi, M., Samoson, A., Engelhardt, G. and Grimmer, A.R. (1980) structural studies of silicates by solid-state high-resolution Si-29 NMR. Jouranl of the American Chemical Society, 102, 4889-4893.

Mackenzie, K.J.D. and Smith, M.E. editor (2002). Multinuclear Solid-state NMR of Inorganic Materials. Pergamon Materials Series, Volumen 6. Amsterdam

Miller, J.M. (1996) Fluorine-19 magic-angle spinning NMR. Progress in Nuclear Magnetic Resonance Spectroscopy, 28, 255-281.

Nigro, E., Crea, F., Testa, F., Aiello, R., Lentz, P. and Nagy, J.B. (1999) The role of alkali cations in the synthesis of Ga-ZSM-5 in fluoride medium. Microporous and Mesoporous Materials, 30, 199-211

Pál-Borbély, G., Beyer, H.K., Kiyozumi, Y. and Mizukami, F. (1997) Recrystallization of magadiite varieties isomorphically substituted with aluminum to MFI and MEL zeolites. Microporous Material, 11, 45-51.

——— (1998) Synthesis and characterization of a ferrierite made by recrystallization of an aluminium-containing hydrated magadiite. Microporous and Mesoporous Materials, 22, 57-68.

Pál-Borbély, G., Szegedi, A. and Beyer, H.K. (2000) Solid-state recrystallization of aluminum-containing kanemite varieties to ferrierite. Microporous and Mesoporous Materials, 35, 573-584.

Pérez-Romo, P., Guzmán-Castillo, M.L., Armendáriz-Herrera, H., Navarrete, J., Acosta, D.R. and Asención Montoya, J. (2003) Synthesis of FSM-16 mesoporous materials: Effect of the anion (F-, Cl-, SO42-) in the ion exchange process on the thermal stability. Langmuir 19, 3446-3452.

Pérez-Romo, P., Guzmán-Castillo, M.L., Armendráriz-Herrera, H., Flores-Rodríguez, R., Navarrete-Bolaños, J. and Montoya de la Fuente, J.A. (2005) Physicochemical properties of FSM-16 modified by fluoride and HPA. Studies in Surface Science and Catalysis, 156, 171-176.

Pinnavaia, T.J. and Johnson, I.D. (1986) A Si-29 MAS NMR-study of tetrahedral site distributions in the layered silicic-acid H^{+}-magadiite ($H_2Si_{14}O_{29}.nH_2O$) and in Na^{+}-magadiite ($Na_2Si_{14}O_{29}.nH_2O$). Journal of Solid State Chemistry, 63, 118-121

Ramdas, S. and Klinowski, J. (1984) A simple correlation between isotropic Si-29-NMR chemical-shifts and T-O-T angles in zeolite frameworks Nature 308, 521-523.

Schaller, T., Dingwell, D.B., Keppler, H., Knöller, W., Merwin, L. and Sebald, A. (1992) Fluorine in Silicate-Glasses - A Multinuclear Nuclear-Magnetic-Resonance Study. Geochimica et Cosmochimica Acta 56, 701-707

Thomas, J.M., Klinowski, J., Ramdas, S., Hunter, B.K. and Tennakoon, D.T.B. (1983) The evaluation of Non-equivalent tetrahedral sites from Si-29 NMR Chemical-Shifts In Zeolites and related Aluminosilicates. Chemical Physics Letters, 102, 158-162.

Wang, G.W., Wu, P. and Tian, Z.G. (2009) Endohedral H-1 NMR chemical shifts of H-2-, H2O- and NH3-Encapsulated Fullerene Compounds: Accurate Calculation and Prediction. European Journal of Organic Chemistry, 1032-1041

Yanagisawa, T., Shimizu, T., Kuroda, K., Kato, C. (1990) The preparation of alkyltrimethylammonium-kanemite complexes and their conversion to microporous materials. Bulletin of the Chemical Society of Japan, 63, 988-992

Yesinowski, J.P., Eckert, H., Rossman, G.R. (1988) Characterization of hydrous species in minerals by high-speed H-1 MAS NMR. Journal of the American Chemical Society, 110, 1367-1375.

Zeng, Q. and Stebbins, J.F. (2000) Fluoride sites in aluminosilicate glasses: High-resolution F-19 NMR results American Mineralogist, 85, 863-867

TABLES

Table 1. Synthesis details and simple names

Sample name	Source of sodium or ammonium[b]	washing
K01[a]	NaOH	water
K01F	NaOH	NaF 0.1M
FK01	NaF	water
FK01F	NaF	NaF 0.1M
K01N	NH_4OH	water
K01NF	NH_4OH	NH_4F 0.1 M
FK01N	NH_4F	water
FK01NF	NH_4F	NH_4F 0.1M

[a] as described by Alba et al. (2006)
[b] $Si/(Na+NH_4)=1$

Table 2. Summary of TG results

	Total x^a	
sample	TG data[b]	NMR data[c]
K01	3.19	3.19
K01F	3.17	3.17
FK01	1.59	2.42
FK01F	1.93	3.08
K01N	1.59	2.87
K01NF	1.13	3.52
FK01N	0.74	3.61
FK01NF	0.79	3.23

[a] According to the formula $NaHSi_2O_5.xH_2O$
[b] temperature range 32º-325º C
[c] corrected from the deconvolution of ^{29}Si(SP) MAS NMR spectra

Table 3. ^{23}Na MQMAS NMR simulation data of kanemite with Si/Na=1

	δ_{iso} (ppm)	C_Q (MHz)	η	%
K01	2.575±0.01	1.956±0.001	0.81	82.00
	-0.592 ±0.003	0.478±0.002	0.10	18.00
K01F	3.049 ±0.008	1.937 ±0.005	0.81	50.90
	2.307 ±0.007	1.643 ±0.001	0.83	23.47
	-0.513±0.003	0.436 ±0.002	0.06	10.24
	-0.219 ±0.003	1.352 ±0.001	0.34	15.39
FK01	3.116±0.009	1.954±0.002	0.82	59.96
	2.721±0.017	1.593 ±0.003	0.84	28.03
	-0.524±0.006	0.336±0.003	0.10	7.08
	-0.306±0.014	1.390±0.004	0.39	4.93
FK01F	2.176 ±0.002	2.041 ±0.003	0.85	39.53
	1.728 ±0.018	1.750 ±0.004	0.86	44.94
	-0.418 ±0.016	0.519 ±0.009	0.10	4.82
	-0.302 ±0.010	1.370 ±0.003	0.33	10.71

Table 4. ^{23}Na MQMAS NMR simulation data of kanemite with Si/(Na+NH_4)=1

	δ_{iso} (ppm)	C_Q (MHz)	η	%
K01	2.575±0.01	1.956±0.001	0.81	82.00
	-0.592 ±0.003	0.478±0.002	0.10	18.00
K01F	3.049 ±0.008	1.937 ±0.005	0.81	50.90
	2.307 ±0.007	1.643 ±0.001	0.83	23.47
	-0.513±0.003	0.436 ±0.002	0.06	10.24
	-0.219 ±0.003	1.352 ±0.001	0.34	15.39
FK01	3.116±0.009	1.954±0.002	0.82	59.96
	2.721±0.017	1.593 ±0.003	0.84	28.03
	-0.524±0.006	0.336±0.003	0.10	7.08
	-0.306±0.014	1.390±0.004	0.39	4.93
FK01F	2.176 ±0.002	2.041 ±0.003	0.85	39.53
	1.728 ±0.018	1.750 ±0.004	0.86	44.94
	-0.418 ±0.016	0.519 ±0.009	0.10	4.82
	-0.302 ±0.010	1.370 ±0.003	0.33	10.71

CAPTIONS OF FIGURES

Figure 1. XRD diagrams of kanemite: a) Si/Na=1 and b) Si//(Na+NH_4)=1. c) Structure of kanemite. T=tridymite and C=cristoballite.

Figure 2. SEM micrographs of: a) K01, b) K01F, c) FK01, and, d) FK01F.

Figure 3. SEM micrographs of: a) K01N, b) K01NF, c) FK01N, and, d) FK01NF.

Figure 4. ^{29}Si (SP) MAS NMR (solid line) and ^{29}Si(CP) MAS NMR (dash line) spectra of kanemite: a) Si/Na=1 and b)Si//(Na+NH_4)=1. c) Relation between the total water content, % w/w, and the proportion of Q^4 environment.

Figure 5. ^{1}H(SP) MAS NMR spectra of kanemite: a) Si/Na=1 and b)Si//(Na+NH_4)=1. c) Relation between proportions of proton involved in hydrogen bonds and proton from water as function of synthesis medium and mineralizing agent.

Figure 6. IR/FT spectra of kanemite: Si/Na=1(left) and Si//(Na+NH_4)=1 (right).

Figure 7. ^{19}F(SP) MAS NMR spectra of kanemite: a) Si/Na=1 and b)Si//(Na+NH_4)=1. *=spinning side bands

Figure 8. ^{23}Na MQ MAS NMR spectra of K01 kanemite.

Fig. 1

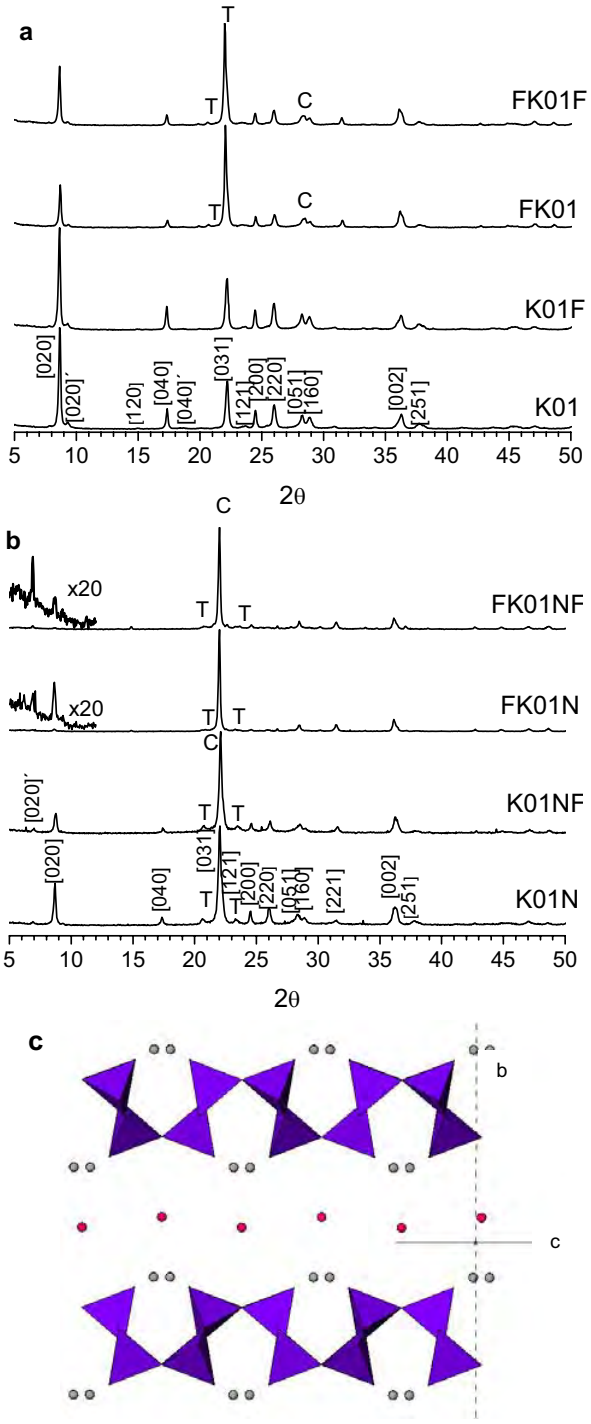

Fig. 2

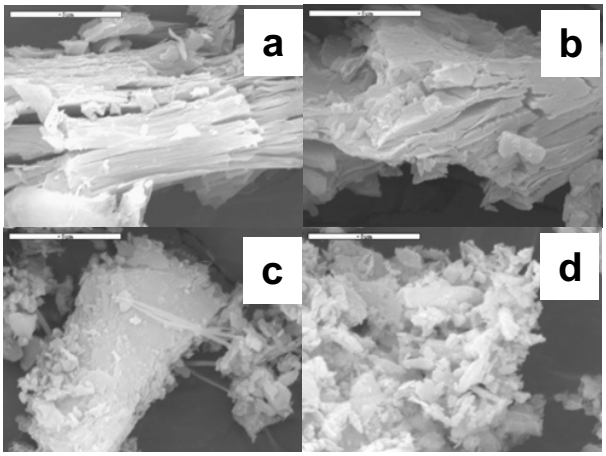

Fig. 3

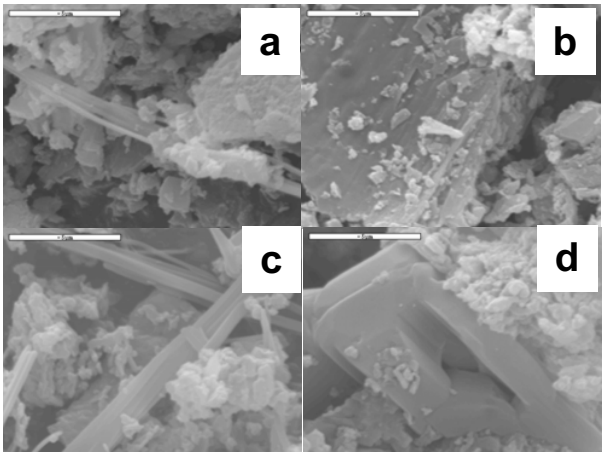

Fig. 4

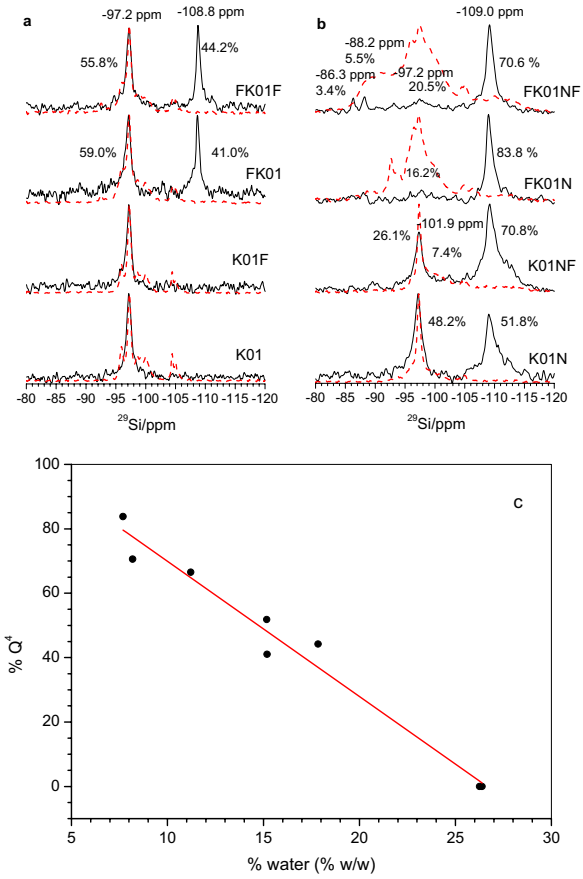

Fig. 5

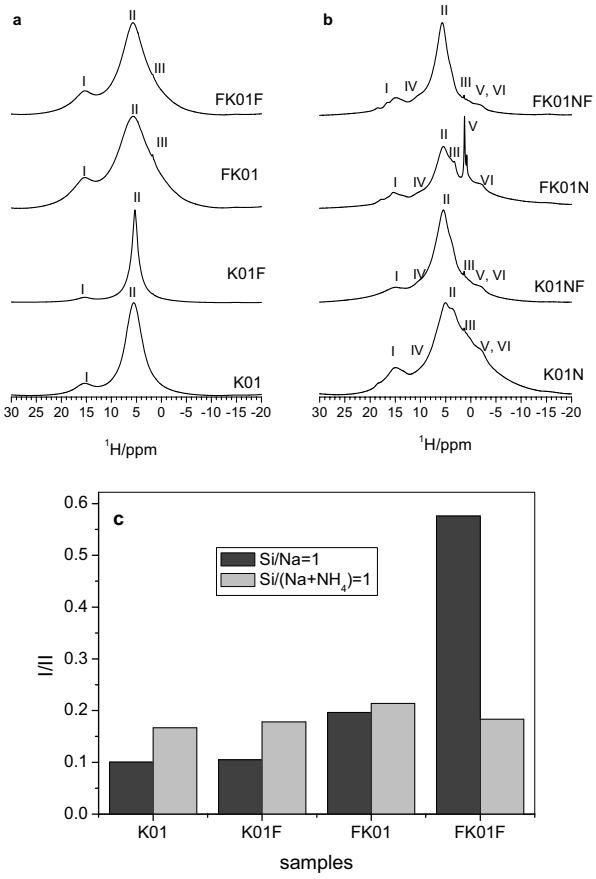

Fig. 6

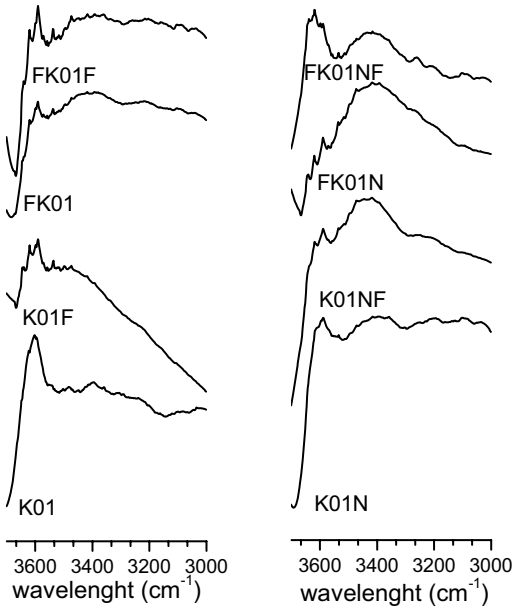

Fig. 7

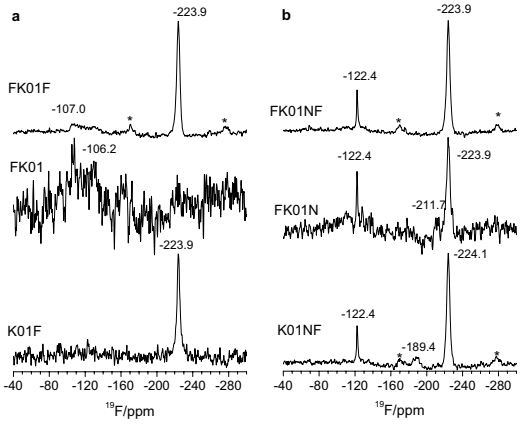

Fig. 8